Oceanologia 63 (2021) 448—462

Available online at www.sciencedirect.com

ScienceDirect

journal homepage: www.journals.elsevier.com/oceanologia

ORIGINAL RESEARCH ARTICLE

Experimental study of hydraulic response of smooth submerged breakwaters to irregular waves

Seyed Masoud Mahmoudof[a,*], **Fatemeh Hajivalie**[a,b]

[a] *Iranian National Institute for Oceanography and Atmospheric Sciences (INIOAS), Tehran, Iran.*
[b] *Ghent University, Department of Civil Engineering, Technologiepark 60, 9052, Ghent, Belgium.*

Received 7 March 2021; accepted 12 May 2021
Available online 27 May 2021

KEYWORDS
Impermeable submerged breakwaters;
Laboratory measurements;
Transmission;
Reflection;
Dissipation

Abstract This paper presents the results of a laboratory experiment on transmission, reflection, and dissipation of irregular waves over smooth impermeable submerged breakwaters. Experiments included 75 JONSWAP-based irregular waves with five different wave characteristics generated at three water depths in a 2D wave flume. The investigated breakwater sections were three rectangular breakwaters with different widths, a toothed rectangular breakwater, and a trapezoidal breakwater with a slope of 1:2.

A new comprehensive dimensionless parameter (β) was proposed representing both wave hydrodynamic and breakwater geometry characteristics. This parameter could be employed as a suitable descriptive option to make an accurate estimate of the hydraulic performances of submerged breakwaters. The β parameter is composed of four conventional simple dimensionless variables. However, the results revealed that the relative submergence depth significantly affects the hydraulic responses of submerged breakwaters. The transmission, reflection and dissipation of waves show a logarithmic growth, a logarithmic reduction, and a quadratic decreasing trend against the increasing of β parameter, respectively. The verifications of results revealed the high efficiency of β parameter for data reported by Carevic et al. (2013) with $R^2 = 0.88$ and high agreement with predictions made by Van der Meer et al. (2005) formulation with $R^2 = 0.93$.

* Corresponding author at: Iranian National Institute for Oceanography and Atmospheric Sciences (INIOAS), Tehran, Iran, 1411813389.
E-mail address: m_mahmoudof@inio.ac.ir (S.M. Mahmoudof).

Peer review under the responsibility of the Institute of Oceanology of the Polish Academy of Sciences.

Production and hosting by Elsevier

https://doi.org/10.1016/j.oceano.2021.05.002

1. Introduction

Coastal areas play an important role in the formation of human civilizations and their strategic activities. The defense of coastal areas against coastal erosion and disasters due to wave impact can improve shoreline stability and can protect some coastal infrastructures such as ports, power plants and refineries (Bao, 2011; Gao et al., 2019, 2020; Kubowicz-Grajewska, 2015). The shoreline erosion and local sediment scour can result in material loss and instability of the foundation of coastal structures (Sumer et al., 2005; Young and Testik, 2011). Different hard protection schemes such as seawalls, revetments, dikes, groins, jetties, near and off-shore breakwaters as well as soft methods such as beach nourishment and sand bypassing are generally implemented to prevent shoreline erosion. Among these types, the gravity-emerged porous rubble mound breakwaters are the traditional type of protective structures and the most efficient ones. Although these breakwaters prevent the waves from reaching the coasts, they obstruct the passage of resident fish and bottom-dwelling organisms. Recently, low crested and submerged breakwaters have been becoming increasingly popular, due to their environmental and economic advantages. The quality of coastal water remains high since fresh water freely circulates through the leeward side of submerged breakwaters. Also, sediment transport is not completely blocked using this type of breakwater. Moreover, they have a low impact on the visual aesthetic of the natural environment, an effect appealing to the tourism industry. So far, many different types of submerged breakwaters have been studied, designed and constructed, such as vertical, inclined, semicircular, rubble mound and blade types. The smooth and impermeable caisson submerged breakwaters are less understood in comparison to the other types.

The breakwaters decrease the wave energy by three mechanisms including wave reflection, breaking, and vortex generating. The submerged breakwaters provide wave attenuation at the leeward side through a partial wave reflection and moderate breaking. The remained wave energy transmits over the breakwater and reaches shore. The influence of submerged breakwaters on some physical and hydrodynamic processes such as sediment transport and water quality has been studied by some researchers (e.g., Lorenzoni et al., 2005). However, the majority of recent studies focused on the transmission, reflection, and dissipation of waves over several types of submerged breakwaters, as well as the spectral wave transformation over them (e.g., Carevic et al., 2012; Fang et al., 2018; Filianoti and Piscopo, 2015; Liu and Li, 2012; Young and Testik, 2011; Zhang et al., 2016). Generally, most of the investigations about wave reflection and transmission have been experimentally conducted and few field measurements can be found (e.g., Davidson et al., 1996; Dean et al., 1997; Mahmoudof and Azizpour, 2020). The accurate estimation of transmission and reflection coefficients provides an efficient and economic design of the height and width of submerged breakwaters which ensures transmission of allowable energy toward the coast and prevents the shore erosion. The submerged breakwaters are so attractive for coastal engineers that the performance of some combined designs of them have been evaluated in some studies (e.g., Liang et al., 2015).

Literature review indicates that different factors (such as water depth at the breakwater position, structure geometry, wave characteristics, and angle of wave strike and distance from the shoreline) affect the efficiency of submerged breakwaters. However, several well-known studies reported that the crest width (B) and freeboard (R_c) are more important than other parameters to explain the hydraulic response of submerged breakwaters to impinging waves (e.g., Goda et al., 1967; Van der Meer, 1991; Van der Meer et al., 2005). The wave height (H), length (L) or water depth (d) were utilized to normalize B and R_c as the descriptive dimensionless parameters in most of the previous studies. For example, Zhang et al. (2016), Young and Testik (2011) and Liao et al. (2013) evaluated the submerged breakwater performance as a function of H/R_c. On the other hand, the works of Suh et al. (2001) and Lokesh et al. (2015) are two examples that presented their results against B/L. Also, considering wave number (k) and period (T), other parameters such as relative depth (kd) and wave steepness (H/gT^2) were regarded as the descriptive variables of submerged breakwater performances (Filianoti and Piscopo, 2015; Liu and Li, 2012; Rageh and Koraim, 2010; Sindhu and Shirlal, 2015). Rao et al. (2009) investigated the influences of Rc/H, d/L, and H/gT^2 on the transmission performance of their studied submerged breakwater. All of these studies have been neglected the collective and associative effects of different factors. Lorenzoni et al. (2016), Van der Meer et al. (2005) and d'Angremond et al. (1996), to the best of our knowledge, attempted to present comprehensive parameters including all the structural geometry factors and wave characteristics to estimate the transmission of structures. However, the performance of these parameters for estimating the reflection and dissipation responses were ignored.

In the present study, it is attempted to find a comprehensive descriptive parameter to estimate all the hydraulic performances (including wave transmission, reflection, and dissipation) of impermeable submerged breakwaters. The study was organized based on experimental observations conducted in a two-dimensional flume.

In the next section, the experimental facilities and wave conditions are represented. The methods of data analysis are explained in Section 3. Experimental observations and results are presented in three subsections of Section 4. Finally, the study is concluded in Section 5.

2. Laboratory facility and experiment procedures

The experiments were performed in a two-dimensional wave flume at the School of Civil Engineering, University of Tehran. Figure 1 shows the flume and experimental conditions schematically. The flume is 26 m long, 1.2 m high and 1 m wide made of transparent 10 mm glass plates. A piston-type paddle is installed at the upstream end of the wave flume which generates both regular and irregular waves. The wave-maker is equipped with an active wave absorption control system (AWACS) to prevent the re-reflection

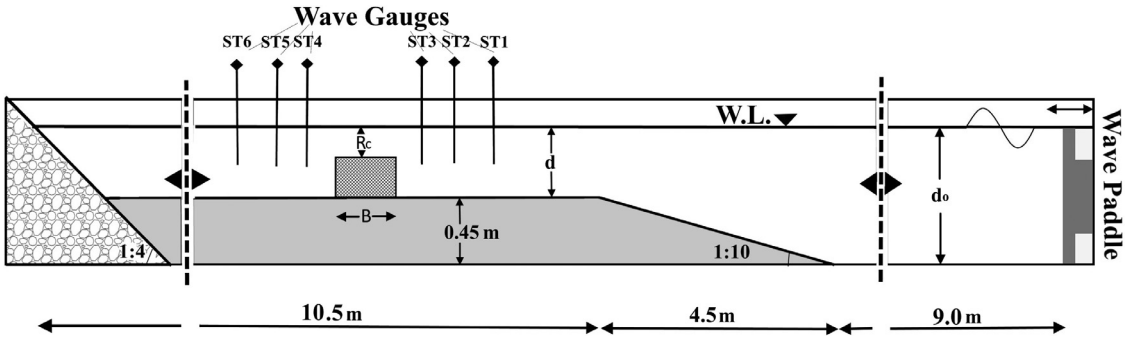

Figure 1 Experimental setup and flume conditions.

of the reflected waves from the experimental structures at the paddle into the flume. This system makes it possible to perform long-time tests without any undesirable wave resonance and growth of wave energy in the flume. At the end side of the flume, a passive wave absorber system consisting of broken stones dissipated the wave energy. In the middle of the flume, a plain slope with an inclination of 1:10 and a height of 45 cm made from masonry materials to increase the ratio of the wave height to the water depth (Figure 1). Normally, this slope results in some wave transformations, such as shoaling or low-frequency energy transmission toward the low and high frequencies due to triad interactions. Although some minor spectral changes could appear, these processes cannot change the spectral peak frequencies.

The experimental waves were generated according to the standard JONSWAP spectrum ($\gamma = 3.3$, $\sigma_a = 0.07$, and σ_b=0.09). The sampling rate was set to 50 Hz at each gauge to record the instantaneous water surface elevation data. Each time the series length was 540 s and sufficient waiting time was applied to permit the wave conditions to dominate in the flume before the measurement started.

Five irregular waves with different peak periods ($T_p = 1.1$, 1.3, 1.5, 1.7, and 1.9 s) and heights were generated at three different deep-water conditions ($d_o = 0.75$, 0.8, and 0.85 m) for each submerged breakwater. These characteristics provided $k_p d$ values between 1.07 and 2.86. All the experimental values of wave steepness ($s_{op} = 2\pi H_i / g T_p^2$) ranged between 0.018 up to 0.055 and less than 0.07. Therefore, all the waves were stable and in the allowable range of wave steepness (Van der Meer et al., 2005). More than 280 waves impinged to the breakwaters in each test. In total, 15 tests with the same periods and depths were conducted for each breakwater section (hereafter BS to avoid confusion with paper structural sections). The experimental hydrodynamic conditions such as wave periods (T_p), wavelength over the structures ($L_{p,s}$), and depths (d and R_c) values are presented in Table 1. The experimental irregular waves experienced combinations of shoaling and probable minor breaking on the inclined bed before impinging to the breakwater. The breakwaters included two main rectangular BSs with 30 and 60 cm width, a toothed rectangular with 60 cm width and two similar right triangular BSs with slopes of 1:2. All the composite experimental BSs and their introducing titles are shown in Figure 2. The height of all breakwaters was 25 cm. It is expected that the energy dissipation due to the viscosity resistance and vortex generation for BS 4 is more than BS 2. The breakwater models were made from impermeable PVC sheets with 1.2 cm thickness. For each test, one of the submerged breakwaters was placed on the masonry platform and wave recording was carried out at the offshore and inshore sides of the breakwater. The independent variables of experimental conditions included significant wave height (H_{m0}), peak period of generated wave (T_p), breakwater width (B), and water depth at structure position (d). The submergence depth ($R_c = 5$, 10, and 15 cm) is the difference between d and structure height. Other wave parameters were calculated according to the implemented analysis methods which will be introduced in the next section. Figure 3 shows BSs 3 and 5 during the experiments.

The test codes for each breakwater were sequenced according to three groups of (ascending) depths with five (ascending) periods. For instance, code 2 represents the experimental waves with the period of 1.3 s and $R_c = 5$ cm, whereas code 14 is representing the waves with the period of 1.7 s and $R_c = 15$ cm.

3. Analysis methods

For each test, the first 40 s data were ignored to ensure that the wave condition was stationary within all flume length. The remaining 540 s long time series of water level data gathered by each wave gauge were processed to obtain the spectral wave parameters. The edges of the time series were smoothed using the Hanning window method. All of the wave characteristics such as wavelength over the breakwater (L) and dependent variables were calculated according to the linear wave theory. Three gauges with 20 and 30 cm distances were installed at the offshore and inshore sides of breakwaters in the range of $0.05 < \Delta l/L < 0.45$ according to Goda and Suzuki (1976) (Figure 1). In that study, one wave-length distance between the reflective surface and the first adjacent gauge was conservatively recommended to avoid fluctuation of irregular standing wave height. However, their results imply somewhat smaller distances can be set to attain this target (as ~0.75 wavelength shown in Figure 6). In the present study, this distance was investigated for long experimental waves ($T_p = 1.9$ s, and $d_o = 0.85$ m) to assure the attaining of a stable negligible fluctuation of the wave height. At the seaward side of the structure, the breakwater was the reflective surface and at the leeward side the passive wave absorber reflected the transmitted waves. The resulted distances were

Table 1 The general experimental hydrodynamic conditions for all BSs and attained results for BS 3 (underlined values).

Test code	d (m)	T_p (s)	R_c (m)	B (m)	L (m)	H_i (cm)	H_t (cm)	H_r (cm)
1	0.3	1.1	0.05	0.9	0.75	4.77	1.10	2.81
2	0.3	1.3	0.05	0.9	0.90	5.95	1.31	3.87
3	0.3	1.5	0.05	0.9	1.02	6.72	1.55	4.64
4	0.3	1.7	0.05	0.9	1.18	7.18	1.80	4.95
5	0.3	1.9	0.05	0.9	1.31	7.74	2.09	5.11
6	0.35	1.1	0.1	0.9	1.03	4.4	2.16	2.16
7	0.35	1.3	0.1	0.9	1.23	5.2	2.29	2.81
8	0.35	1.5	0.1	0.9	1.44	5.71	2.46	3.14
9	0.35	1.7	0.1	0.9	1.64	6.35	2.79	3.43
10	0.35	1.9	0.1	0.9	1.85	6.66	2.93	3.53
11	0.4	1.1	0.15	0.9	1.22	4.36	2.75	2.09
12	0.4	1.3	0.15	0.9	1.48	4.99	3.14	2.25
13	0.4	1.5	0.15	0.9	1.74	5.79	3.36	2.55
14	0.4	1.7	0.15	0.9	1.99	6.14	3.68	2.58
15	0.4	1.9	0.15	0.9	2.24	6.81	4.09	2.86

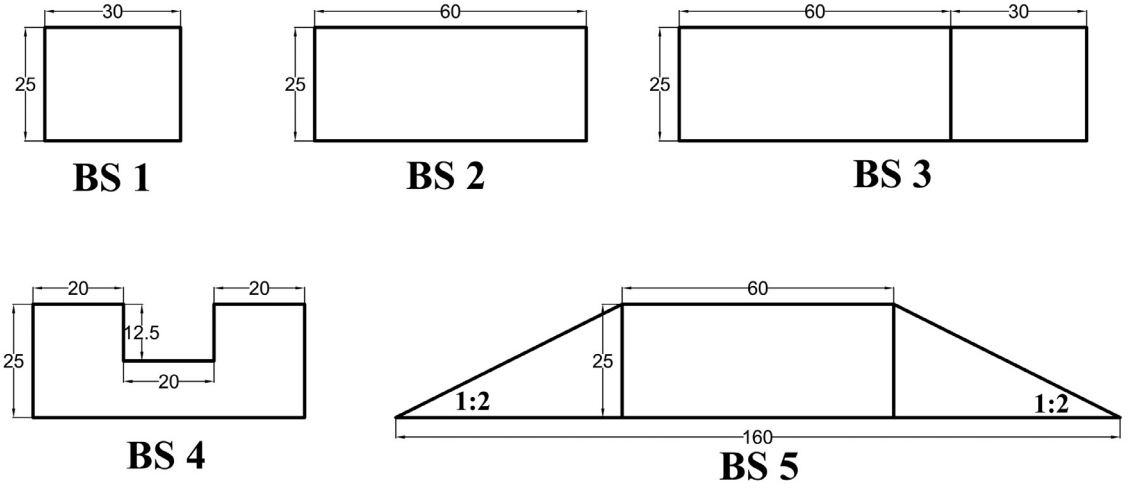

Figure 2 The experimented BSs and their titles. All dimensions are in centimeter.

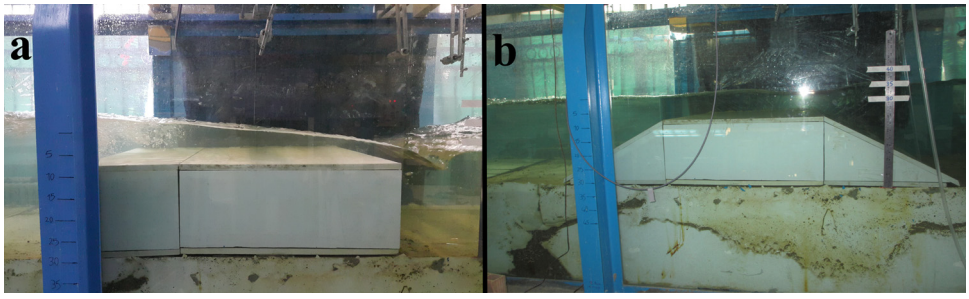

Figure 3 Two BSs during experiments: a) BS 3; b) BS 5.

greater than 0.8 of a wavelength and in agreement with the results of Goda and Suzuki (1976). All of the gauges were positioned at the middle point of flume width to prevent probable asymmetrical influencing factors. For most cases, Mansard and Funke (1980) method was implemented on the synchronized data to separate the incident and reflected waves at both sides of structures. Also, the Goda and Suzuki (1976) method was implemented in the rare cases that one gauge failed to work properly.

The transmission (K_t) and reflection (K_r) coefficients are two important hydraulic variables for submerged breakwater and are calculated as follows:

$$K_t = \frac{H_t}{H_i} \tag{1}$$

$$K_r = \frac{H_r}{H_i} \tag{2}$$

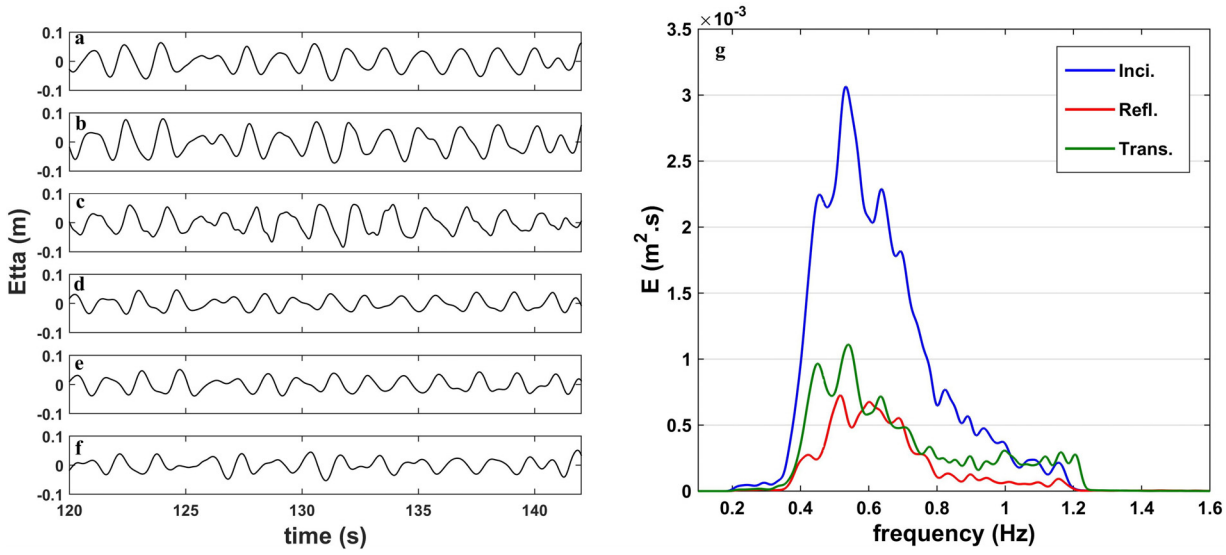

Figure 4 A short part of a long time series of water level fluctuations at offshore side: a) ST1, b) ST2, c) ST3, and inshore side: d) ST4, e) ST5, and f) ST6, g) spectra of incident, reflected and transmitted waves of test #15 of BS 1 with d=40 cm.

where H_i, H_t and H_r denote the incident, transmitted, and reflected wave heights, respectively. Another important breakwater hydraulic variable is energy dissipation rate defined as follows:

$$K_d = 1 - K_t^2 - K_r^2 \tag{3}$$

The values of these three parameters are normally in range of 0—1.

4. Results and discussions

4.1. Basic observations and results

The measured data pertained to 3 rectangular and toothed BSs (BSs 1—4) were processed to describe the general hydraulic functions of studied breakwaters. Figure 4 shows a short part of a full synchronized time-series of water level fluctuations at 6 stations and relevant energy spectra of incident, reflected and transmitted waves for test no. 15 of BS 1 with $d = 40$ cm. The incident, reflected, and transmitted wave heights were primarily determined. Table 1 shows general experimental conditions and all of the measured parameters pertaining to BS 3 as an example. A rough evaluation of the ratio of H_i/d reveals that the experiments included waves with different nonlinearity degrees. Therefore, wave breakings with different intensities have occurred over the breakwaters. Generally, highly nonlinear waves experience more intensive wave breaking than linear waves resulting in relatively lower wave transmission.

It was preliminary revealed that the differences between the performances of BSs 2 and 4 are negligible. This is a convincing evidence of reliability and repeatability of experiments. A possible explanation for this finding may be the same dimensions of vertical face against incident wave which result in more significant energy loss caused by wave breaking and reflection than the dissipation pertaining to vortex generating (Hajivalie et al., 2015).

Most similar experimental studies have concentrated on the estimation of the hydraulic responses of breakwaters (transmission, reflection, and dissipation) based on the main hydrodynamic parameters representing the wave and structure characteristics. The dimensionless forms of these suggested parameters are preferred to represent their general descriptive effect. As mentioned, the suggested dimensionless parameters included relative submergence depth (R_c/H_i), relative crest width (B/L and B/H_i), relative submergence depth (R_c/d), local and offshore wave steepness (H_i/L and H_o/gT^2), and relative depth (d/L). In the first stage of the present study, the influence of these parameters accompanied by a rarely used parameter (R_c/B) on wave transmission, reflection, and dissipation was investigated. The transmission and reflection coefficients were calculated using Eqs. (1) and (2), respectively. The results are demonstrated in 16 panels of Figure 5. The blue, red, and green markers in the panels a to n are introducing the water depth at breakwater position (d) as 30, 35, and 40 cm (or R_c as 5, 10, and 15 cm), respectively. Also, square, circle, diamond, and pentagram markers in panels a to l represent the submerged breakwater BSs 1 to 4, respectively. In addition, each broken line in panels m and n are showing the variations of K_t and K_r as a function of R_c/B for given T_p and d values (each broken line is representing the results of tests with the same conditions pertaining to four BSs). Similarly, the broken lines in the panels o and p are representing the trends of K_t and K_r as a function of R_c/d for tests with similar T_p and B values (each broken line is representing the results of tests with the same periods at three water depths pertaining to each BS). In the last four panels, the effect of incident wave height differences between connected points was only ignored (the maximum deviation of incident wave height for each group was about 12%). The remarkable finding emerging from these figures is that data were categorized into three separated groups corresponding to water depth value. This event prevents obtaining a unique relationship to estimate the hydraulic responses of structure in different conditions. Also, the results of some

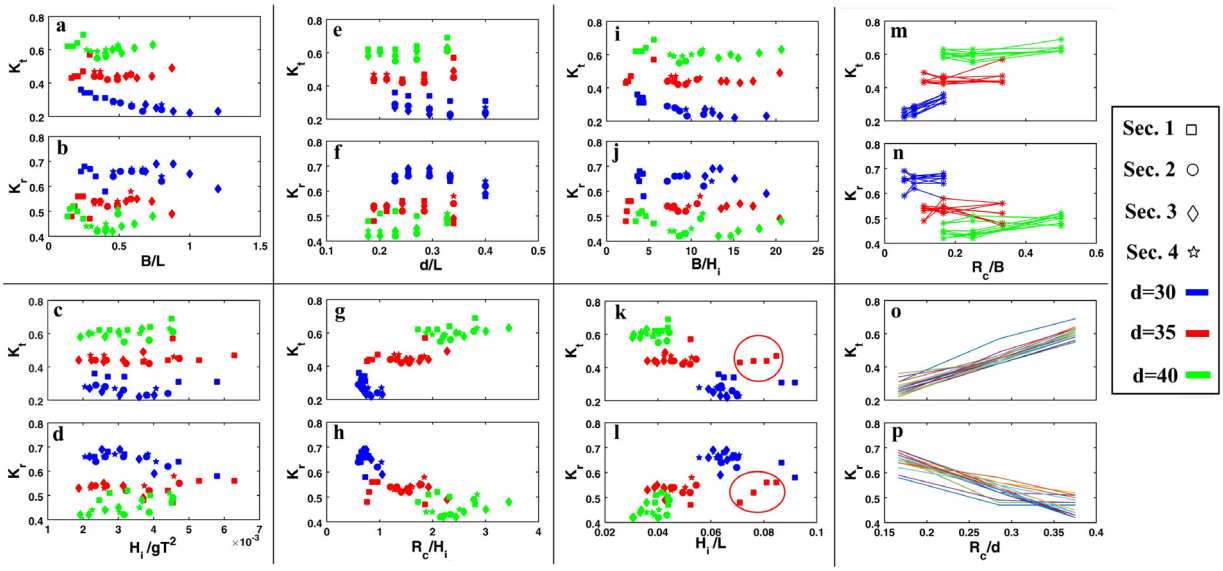

Figure 5 Variations of transmission (K_t) and reflection (K_r) coefficients against: a) and b) B/L, c) and d) H/gT^2, e) and f) d/L, g) and h) R_c/d, i) and j) B/H_i, k) and l) H_i/L, m) and n) R_c/B, o) and p) R_c/d. The blue, red and green symbols are pertaining to local water depth of 30, 35 and 40 cm, respectively. Also, square, circle, diamond, and pentagram-stars markers show the results for BSs 1—4 in panels a)—l), respectively.

tests carried out with the water depth of 35 cm were mixed with the results pertaining to those of 40 cm (panels a, b, f, g, h, l, m, and n). On the other hand, some points are far away from their corresponding water depth cloud data as shown with two hollow circles in panels k and l of Figure 5.

It is apparent from Figure 5 that the dependency of K_t and K_r on R_c/d values is significantly sensitive. Also, the responses of K_t and K_r to R_c/H_i, H_i/L and R_c/B variations are evident. However, the intensity of these responses against each parameter is not similar for three experimental water depths. For example, the influence of R_c/B variations on K_t for the experimental water depth of 30 cm is more substantial than two other water depth values.

As expected, the responses of K_t and K_r to these dimensionless parameter variations are generally opposite to each other. While K_r represents a negative correlation with the growth of R_c/d, the positive correlation of K_t with R_c/d is evident (Figure. 5o and p) and consistent to Dattatri et al. (1978). Lorenzoni et al. (2016) considered the effect of relative submergence depth as the ratio of submerged breakwater height to water depth in their proposed determinative dimensionless parameter (χ in that study). In agreement with the present study, they found a positive correlation of transmission coefficient with R_c/d variation parameters.

The increment of K_t and decrease of K_r against the growth of R_c/H_i (Figure 4g and h) is in perfect agreement with some previous studies. Zhang et al. (2016) found the growth of K_t against the rise of R_c/H_i for smooth submerged breakwater using the SWASH model. Young and Testik (2011) found two similar descending trends of the reflection coefficient versus R_c/H_i increasing for vertical and semicircular submerged breakwaters. The findings of Bleck and Oumeraci (2002) implied the ascending trend of K_t for R_c/H_i growth. Moreover, Rao et al. (2009) showed the positive correlation of wave transmission over submerged inclined plate breakwaters with increasing R_c/H_i for relative depth values greater than 0.12.

Rageh and Koraim (2010) installed vertical walls with horizontal slots to model the breakwater structure in their experimental investigation. They reported descending K_t and ascending K_r values against the increase of wave steepness (H_i/L), which is consistent with the results obtained in the present study (Figure 4k and l). Also, Lorenzoni et al. (2016) identified the wave steepness parameter as the most effective factor (with the exponent of 3) and showed the inverse correlation of K_t with (H_i/L).

In contrary to the aforementioned attained correlations and dependencies, no considerable sensitivity of K_t or K_r to B/L, H_o/gT^2, d/L, and B/H_i was found in each data group (water depth category). Although K_t variations versus B/L were nearly descending for the water depth of 30 cm, no significant dependency was observed for two other depth values (Figure 5a). This could be due to the increment of wavelength for a given period as a result of increasing submergence depth (R_c) and the decrease of B/L of breakwaters, consequently. Therefore, the parameter of B/L is ineffective for high values of R_c (in agreement with previous studies such as Hajivalie and Mahmoudof, 2018). In agreement with this finding, Lorenzoni et al. (2016) considered a slight influence for B/L, assigning the exponent of 0.5 in their proposed determinative parameter (compared with the exponent of H_i/L as 3). Also, the negligible variations of K_t and K_r against d/L in each water depth group could be interpreted with a similar explanation. Consistent with the present study (Figure 5i), Zhang et al. (2016) results showed a very mild variation of K_t against B/H_i.

However, some researchers have different opinions. Suh et al. (2001) reported that in perforated-wall caisson breakwaters, the minimum values of frequency-averaged reflection coefficients corresponded to $B/L \sim 0.2$. Lokesh et al. (2015) investigated smooth and step sub-

merged breakwaters with different ranges of R_c/H_i and crest width values and reported a mild descending trend of K_t values against increasing of B/L parameter in agreement with Dattatri et al. (1978) results. The R_c/H_i values ranged between 1.4 and 4.64 and three widths of 10, 20 and 30 cm were applied in a constant water depth of 31 cm in Lokesh et al. (2015). Also, in the Dattatri et al.'s (1978) study, the values of R_c/d and B/L were less than 0.4 and 0.7, respectively. The water depth was also constant in the investigation of Dattatri et al. (1978), and was equal to 50 cm. Although the position of wavelength calculation in Dattatri et al. (1978) was somewhat different from that of the present study, the above-mentioned parameter ranges in their studies were relatively equal with those of the present study. However, three trends of mild decreasing, senseless, and mild increasing of K_t for increasing of B/L values have been found in the present investigation for water depths of 30, 40, and 50 cm, respectively. Therefore, the associative effects of all influencing factors in the different water depths can be responsible for these different found results.

Fang et al. (2018) and Liu and Li (2012) paid attention to the relative depth as the main important parameter influencing the hydraulic performances of submerged breakwaters. Similar to Filianoti and Piscopo (2015), they evaluated the reflection, transmission, and dissipation of impinging waves to their studied submerged breakwater as functions of d/L parameter. Rao et al. (2009) found that K_t values decreased against the increase of d/L for horizontal plate installed as a submerged breakwater. Also, they reported a descending trend of K_t as a function of offshore wave steepness (H_o/gT^2), in agreement with Sindhu et al. (2015).

The dissipative efficiency of each BS in each test was evaluated using Eq. (3). The dependency of K_d on four characteristic parameters stabilized in the present study are depicted in Figure 6. As in Figure 5, different colors in Figure 6c indicate different experimental water depths and broken lines in Figure 6d pertain to experiments with the same BS and peak period. It could be found from this figure that the variations of K_d against R_c/d and R_c/H_i are more significant than those of two other parameters (Figure 5a and d). A downward open quadratic curve is the best-fitted line of scatter data of energy dissipation rate as a function of R_c/H_i.

4.2. Introducing a new descriptive parameter

Classic investigations revealed that R_c/H_i, H_i/L_p, and R_c/B were effective on K_t and K_r values and R_c/d had the most significant controlling role in K_t and K_r variations. On the other hand, no unique curve could be fitted to the all of scattered data of K_t and K_r against these simple parameters. Also, the results were mostly categorized by the experimental depths of water. In this study, attempts have been made in order to define a new comprehensive dimensionless parameter (representing the effects of all simple aforementioned parameters) that governs the variations of K_t and K_r. Using this probable parameter, the variations of K_t or K_r must be estimated using a unique trend regardless of the specific physical conditions of each test, such as water depth.

It was supposed that the desirable parameter (β) is a function of four simple effective parameters as follows:

$$\beta = f\left(\frac{R_c}{d}, \frac{R_c}{H_i}, \frac{H_i}{L_p}, \frac{R_c}{B}\right) = \left(\frac{R_c}{d}\right)^{\alpha}\left(\frac{R_c}{H_i}\right)^{\gamma}\left(\frac{H_i}{L_p}\right)^{\lambda}\left(\frac{R_c}{B}\right)^{\kappa} \quad (4)$$

All of the above two-termed fractional expressions are independent of each other except $\frac{R_c}{H_i}$ and $\frac{H_i}{L_p}$ since L_p is dependent on wave period and R_c. However, L_p is more effectively controlled by wave period than R_c and reflects the local influence of wave period as another independent and primary parameter. Since the variations of K_t and K_r were mostly opposite each other (Figure 5), the transmission coefficient was focused to determine the exponents of each dimensionless parameter in Equation (4). The above findings (illustrated in Figure 5) showed that the value of α must be positive and greater than γ and κ, whereas, λ must be negative. Primary evaluations revealed that a logarithmic relationship could be considered as the best-fitted line between K_t values and β parameter. Then, it was attempted to minimize the error of the fitted line and to attain the highest possible R-squared parameter value. According to a vast trial and error process, as well as considering an engineering accuracy and application, the values of α was supposed to be equal to one as the exponent of the most effective parameter and other exponents were determined as $\gamma = 0.5$, $\kappa = 0.5$ and $\lambda = -0.5$. Therefore, β is introduced as follows:

$$\beta = \frac{R_c^2 L_p^{0.5}}{dH_i B^{0.5}} \quad (5)$$

Assuming the shallow water condition ($L_p = T_p.\sqrt{gR_c}$, where g is the gravitational acceleration and T_p is the peak period of the irregular wave) on the crests of breakwaters, another representation of Eq. (5) can be deduced as follows, in which all of the physical parameters are independent from each other:

$$\beta = \frac{g^{0.25} R_c^{2.25} T_p^{0.5}}{dH_i B^{0.5}} \quad (6)$$

The scatter diagram of K_t as a function of β is illustrated in Figure 7a. However, the data grouping according to the water depth remained somewhat similar to two-term parameters (Figure 5), but an excellent unique ascending logarithmic trend was a result showing the best-fit line of K_t as a function of β with $R^2 = 0.97$ (Figure 7a). However, the deviations of K_t values from the best-fitted line for low β values are more considerable than those for high β values. This finding indicates that the β parameter is probably more efficient for waves with low nonlinearity degrees and moderate wave breaking intensities. On the other hand, a descending logarithmic trend was discovered for K_r against β with $R^2 = 0.86$ (Figure 7b). The formulae of fitted curves to estimate the K_t and K_r values are presented as follows, respectively.

$$K_t = 0.149 \ln(\beta) + 0.59 \quad (7)$$

$$K_r = -0.084 \ln(\beta) + 0.47 \quad (8)$$

Replacing Eq. (5) with Eq. (6) has no impact on the fitted curve relationships and deviations. Here, some explanations about the physical influence of the β parameter on K_t and K_r are given provided that only one parameter is

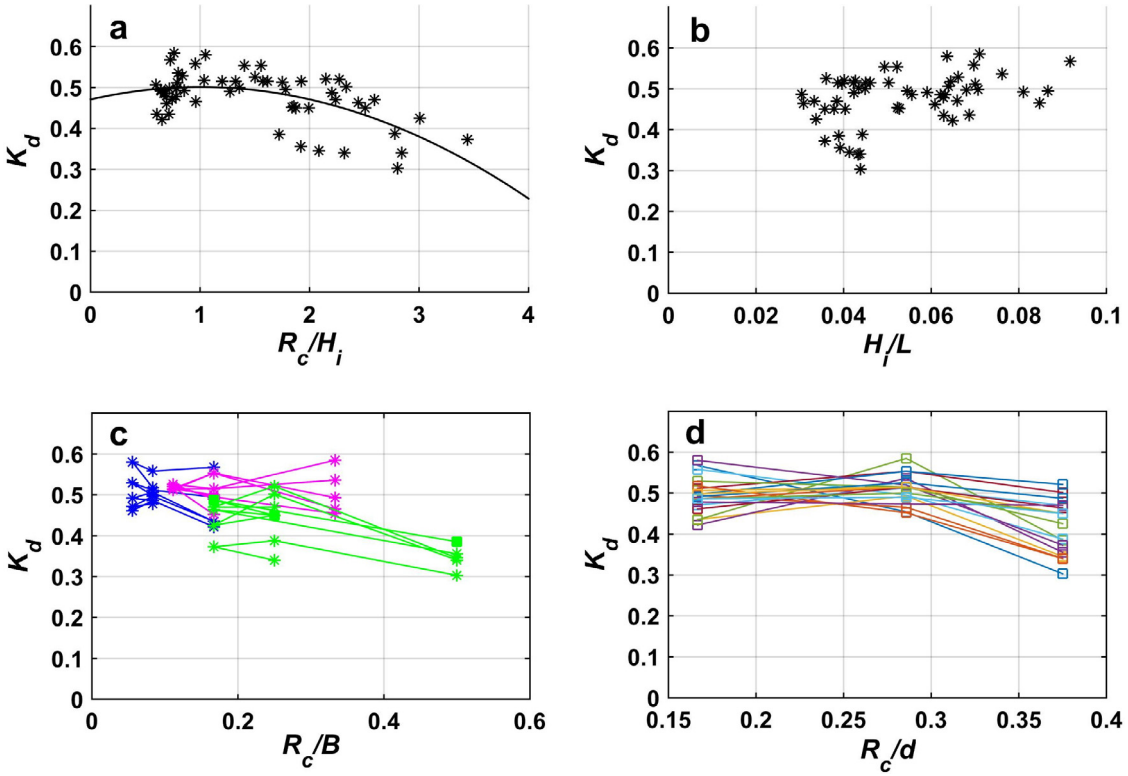

Figure 6 Variations of dissipation coefficient against: a) R_c/H_i, b) H_i/L, c) R_c/B and d) R_c/d.

variable. Suppose that all the breakwater geometries and wave characteristics are constant and the wave height is the only variable parameter. The increase of H_i values leads to the mathematical decrease of β value (see Eq. (5) or (6)) and to reduction and increase of K_t and K_r values according to Eqs. (7) and (8) or Figure 7a and b, respectively. These variations can be physically explained by more intensive interaction between wave and structure. More intensive wave breaking due to the increase of H_i/d dissipates more energy content and decreases height of the transmitted wave. Therefore, this dissipation leads to the decrease in K_t values. Although the majority of the energy content of a short incident wave transmits over a submerged breakwater, the reflection and dissipation of a high wave impinging with the same breakwater are more significant than transmission. Therefore, K_r value corresponding to a high wave is greater than that of a short wave. Moreover, the reduction of R_c value against the immutability of other parameters resulting in the decrease of β parameter can affect the same way the increase of H_i. Also, the growth of B/L_p ratio which decreases the β parameter can result in more dissipation of the transmitting wave reducing the K_t value.

From Eqs. (7) and (8), it could be realized that the variations of K_t are approximately two times more sensitive than those of K_r to $\ln(\beta)$. While the observed β values ranged between 0.13 and 1.5, this parameter could be variable in a wide range of 0.03–22.66 to satisfy the condition of $0 < (K_t, K_r) < 1$ according to Eqs. (7) and (8).

The scatter diagram of K_d as a function of β is illustrated in Figure 7c. It could be found that the peak values of K_d resulted from $\beta \approx 0.4$ and the values of K_d decreased against an increase of the β values greater than 0.4. The β values corresponding to the peak K_d values are dependent on the intrinsic reflection characteristics of the structure material. However, a downward open quadratic curve (similar to Figure 6a) was evaluated as the best-fitted curve of scattered K_d values against β. This trend estimates the K_d values more accurately for the higher values of β than the lower ones. Since the β parameter is calibrated for K_t values, this parameter can estimate the K_t values more accurately than the values for K_r. Therefore, the gathering of all low inaccuracies of K_t and K_r together results in more considerable inaccuracies of K_d than K_t and K_r, especially for low values of β parameter. Rageh and Koraim (2010) found a similar quadratic curve for K_d as a function of H_i/L_p. Also, Liao et al. (2013) concluded a sharp descending trend of residual wave energy ($E_r = {K_r}^2 + {K_t}^2$) versus H_i/R_c for submerged porous breakwaters.

It could be found that not only the parameterization of β is uncomplicated, but also its capability to predict the values of K_t, K_r, and K_d is statistically significant. Interestingly, the faraway results from their corresponding depth data clouds (pointed out in the last subsection in Figure 4k and l) are completely removed from irrelevant data group based on using the β parameter, and they are compatible with the fitted curves. This parameter could describe the hydraulic properties of investigated breakwaters in different wave characteristics as well as rectangular breakwater geometries. Three aforementioned performances of submerged smooth impermeable breakwaters can be predicted simply by using Eq. (5).

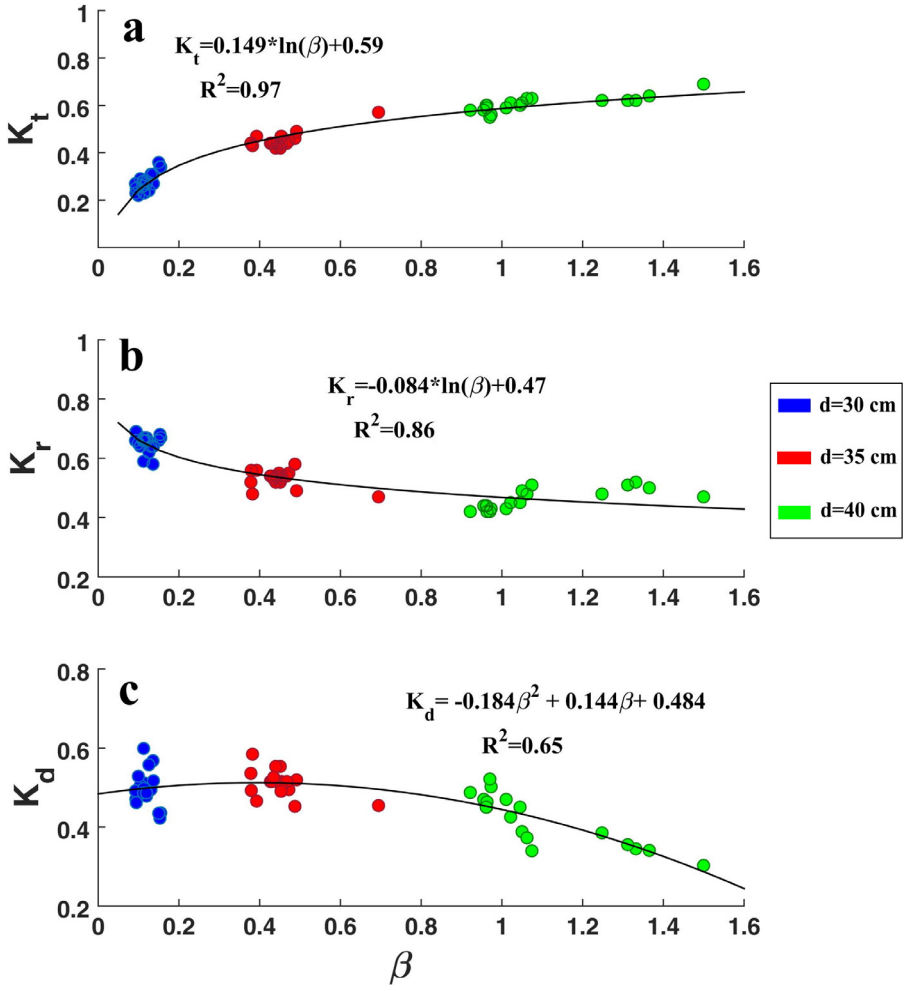

Figure 7 The capability of proposed coefficient (β) to predict the a) transmission, b) reflection and c) dissipation coefficients and their fitted line equations for BSs 1—4.

4.3. New parameter reliability and capability

Now, the capability and reliability of the newly introduced descriptive parameter (β) are assessed against similar data acquired from a trapezoidal submerged breakwater with symmetrical slopes of 1:2 (BS 5). All experimental characteristics were similar to the previous four BSs. In the calculations, the upper side of trapezoidal BS was considered as the width of the breakwater (B). The results, including the wave transmission, reflection, and dissipation coefficients, are illustrated in Figure 8. Surprisingly the performance of β for BS 5 was better than for the rectangular BSs, with superior correlation coefficients and R-squared values. The equations of fitted line to K_t and K_r values for trapezoidal BS were evaluated as follows:

$$K_t = 0.223\ln(\beta) + 0.79 \tag{9}$$

$$K_r = -0.088\ln(\beta) + 0.43 \tag{10}$$

According to Eqs. (9) and (10), the β parameter can range between 0.04 up to 3.75, theoretically. Comparing Figures. 4 and 5 with 6 and 7 reveals that the new dimensionless hydrodynamic parameter undoubtedly improves the estimation of hydraulic response factors of investigated submerged breakwaters. The coefficients and exponents of fitted curve equations pertaining to trapezoidal BS differentiate from those of rectangular BSs due to geometrical differences. However, the equations of fitted curves due to reflection coefficients are very close together Eqs. (8) and (10). The only disagreement was found in a fitted upward open quadratic curve to K_d values which was close to a straight line. Certainly, other features of trapezoidal BSs such as front and behind slopes are affecting their hydraulic properties (Liao et al., 2013).

This investigation indicated the capability and reliability of utilizing β to estimate the reflection, transmission, and dissipation coefficients of the smooth impermeable submerged breakwaters. Also, no exceptive supposition such as water depth, Rc/B, or Rc/d categories was necessary to determine the trends of K_t, K_r, and K_d.

For more assurance of β parameter performance, the presented experimental data and found formulation for K_t were verified with formulae of Van der Meer et al. (2005) and the measurements of Carevic et al. (2013). Van der Meer et al. (2005) recommended to calculate the transmission coefficients of smooth low crested structure, having a trapezoidal BS, with $\frac{B}{H_i} < 10$ using the following re-

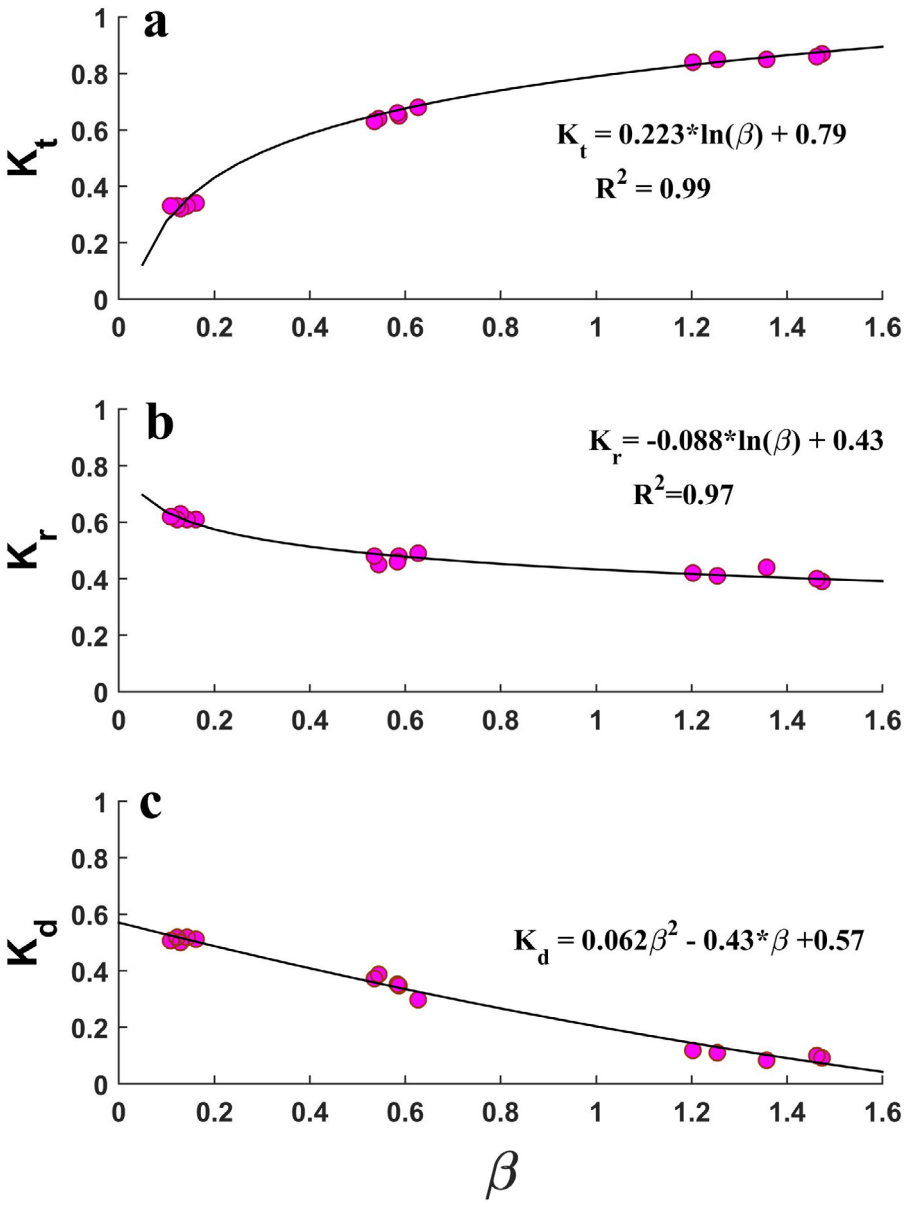

Figure 8 The capability of proposed coefficient (β) to predict the a) transmission, b) reflection and c) dissipation coefficients and their fitted line equations for BS 5.

lationships:

$$K_t = -0.4\frac{R_c}{H_i} + 0.64\left(\frac{B}{H_i}\right)^{-0.31}(1 - e^{-0.5\xi}) \quad (11)$$

In that study, Eq. (11) was modified for $\frac{B}{H_i} > 10$ as follows:

$$K_t = -0.35\frac{R_c}{H_i} + 0.51\left(\frac{B}{H_i}\right)^{-0.65}(1 - e^{-0.41\xi}) \quad (12)$$

with the upper limit of

$$K_{tu} = -0.006\frac{B}{H_i} + 0.93 \quad (13)$$

where $\xi = \frac{\tan\alpha}{\sqrt{2\pi H_i/gT^2}}$ is the well-known wave breaker parameter in Eqs. (11) and (13). The most pressing issue in the application of Eqs. (11)–(13) is discontinuity of K_t values in the range of $8 < \frac{B}{H_i} < 12$. Van der Meer et al. (2005) recommended linear interpolation between values attained using Eqs. (11) and (12) in this range. In the present study, the values of $\frac{B}{H_i}$ varied between 7.5 and 15.6 for trapezoidal breakwater (BS 5). The comparison between the present measured K_t values, their fitted curve, and the predicted values by Van der Meer et al. (2005) is presented in Figure 9. It can be found that the estimations of Van der Meer et al. (2005) are generally in a good agreement with measured K_t values with $R^2 = 0.93$. For high values of β parameter ($R_c = 15$ cm) the predicted values by Eqs. (11) and (12) are not reliable and the values resulting from Eq. (13) must be replaced which is in strong agreement with measured values in the present study.

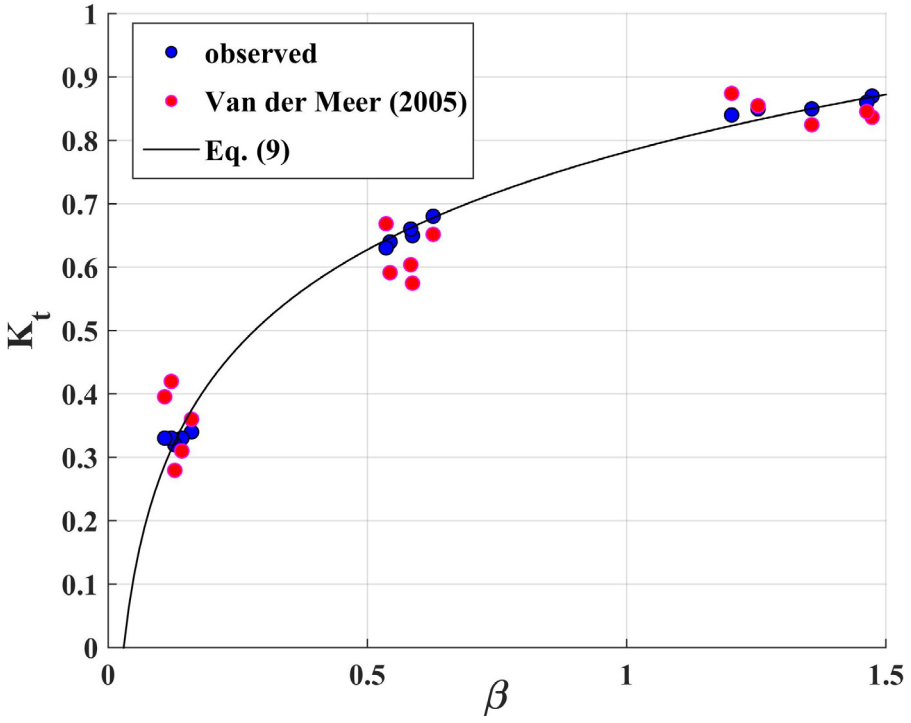

Figure 9 The comparison between observed K_t, fitted curve and predicted values by Var der Meer et al. (2005).

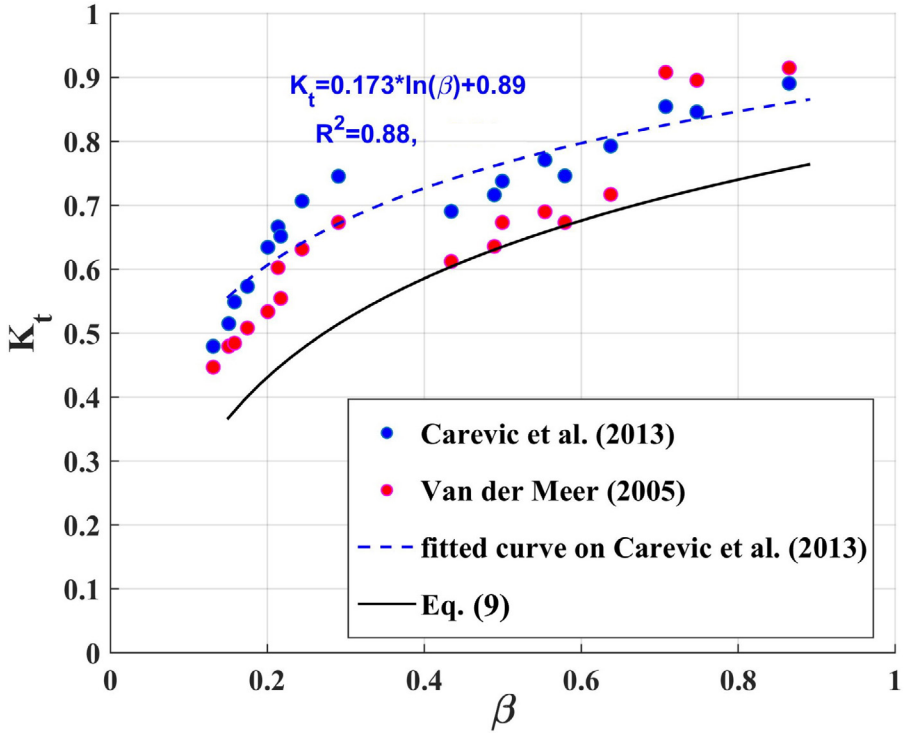

Figure 10 The capability of β parameter for measurements of Carevic et al. (2013) and comparison with Eqs. (9) and (11)–(13).

Moreover, the reliability of the β parameter was evaluated using data of Carevic et al. (2013) study. These data were extracted from Table 1 and Figure 1 of that paper. The breakwater had a trapezoidal BS with an upper width of 16 cm and symmetrical slope of 1:2. Eighteen tests were conducted with experimental waves generated according to JONSWAP spectrum with 9 peak periods at 2 different water depths. All the experimental $\frac{B}{H_i}$ values were less than 3 for that study. The calculated values of the β parameter were ranged between 0.15 and 0.86 for that study. The K_t values are plotted against β parameter and a logarithmic curve as the best-fitted line is shown in Figure 10 for observations of

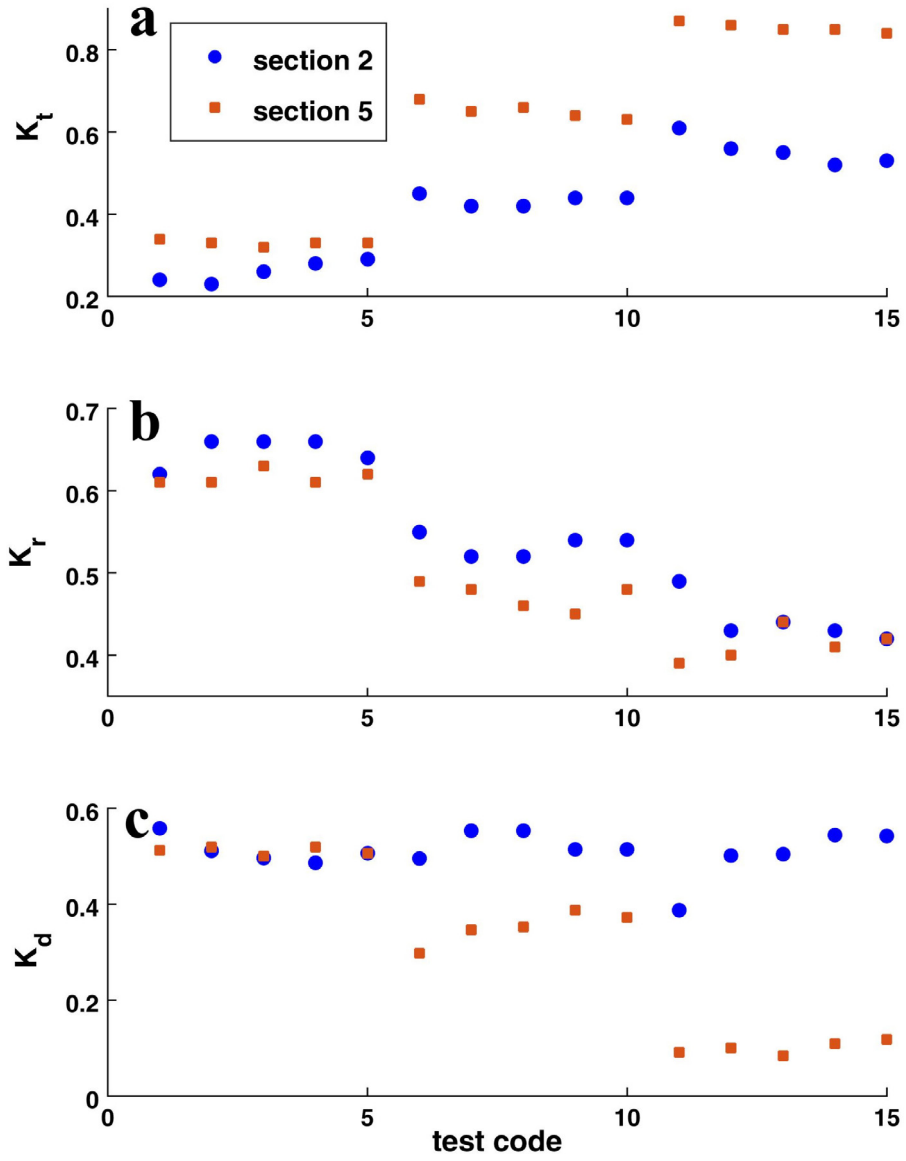

Figure 11 Comparison the: a) transmission, b) reflection and c) dissipation of BSs 2 (circles) and 5 (squares).

Carevic et al. (2013). The formulation of best-fitted curve is as follows.

$$K_t = 0.173 * \ln(\beta) + 0.89 \quad (14)$$

The high values of 0.91 as the correlation coefficient and 0.88 as the R-squared parameter indicate the capability of β and confirm that using this parameter for Carevic et al. (2013) data set is also reliable. However, with the growth of β values up to 3.75 (as observed in the present study) the fitted trend predicts defective values of K_t greater than unity (~1.1). As depicted in Figure 10, for β values ranged between 0.4 and 0.65, Van der Meer et al. (2005) formulations Eqs. (11)–(13) predict lower K_t values for data set of Carevic et al. (2013) in a very strong agreement with the found fitted curve in the present study (Eq. (9)).

These investigations revealed the high capability of the β parameter. A single logarithmic formulation of β parameter can predict the values of K_t without any discontinuity and shows a good agreement with three- formulation relationship of Van der Meer et al. (2005). Although the β parameter was calibrated for transmission coefficient, the fitted curve to the measured K_r values as a function of β showed unimportant and acceptable deviations. However, the calibration of β parameter for reflection coefficients using another data set with similar experimental conditions and merging with the calibration for K_t can improve the results in the probable future studies.

4.4. Breakwater comparison and full-scale application

The hydraulic performance of two wedges was assessed by comparing obtained results for BSs 2 and 5. Although insignificant differences between their reflective functions were found, the differences between their transmission and dissipative performances increased with increasing water

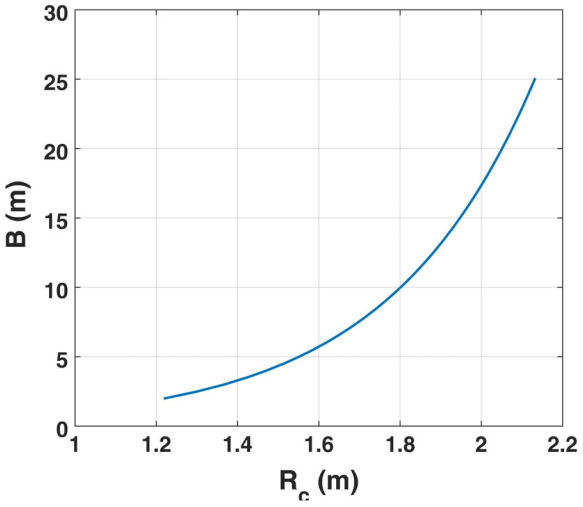

Figure 12 The variation of B against R_c for the assumed submerged breakwater conditions.

depth (Figure 11). The averaged transmission coefficient of BS 2 was approximately 30% less than that of BS 5 at the water depth of 40 cm. This superiority of BS 2 also resulted in approximately 40% more effective energy dissipation than that of BS 5. It should be noted that the better efficiency of BS 2 has been obtained with an economic benefit by approximately 45% reduction in breakwater volume compared to BS 5.

Now, a full-scale rectangular submerged breakwater could be theoretically designed according to the proposed β parameter (Eq. (5)). Assuming that all the hydrodynamic conditions and dimensions are in a rational and normal range, thus, the incident wave at the offshore side has a 1.5 m height with a period of 10 s. The maximum allowable wave height at the leeward is 0.75 m and water depth at the structure position is selected as 5 m. Accordingly, the transmission coefficient is equal to 0.5 and the corresponding β value from Figure 7a is about 0.6. The wavelength values over the structures are computed as a function of R_c according to linear wave theory. Finally, a theoretically wide range of B values against R_c variations is obtained as Figure 12 which results in $\beta \sim 0.6$. However, this study is based on two-dimensional experiments and some other three-dimensional features such as wave attack direction can influence the attained results in the present study. In practice other factors such as tidal range, economic, environmental, and sedimentary concerns will dictate design features. Also, hydraulic and structural stabilities must be checked. Therefore, the hydraulic response of breakwater presented in Figure 12 as well as other design limitations should be taken into consideration to obtain the best geometrical dimensions for this submerged breakwater.

5. Conclusion

In this paper, a laboratory apparatus was implemented to investigate the hydraulic response of impermeable submerged breakwaters to irregular waves. The experimental breakwaters included three rectangular sections with three different widths (B), one toothed rectangular, and one trapezoidal section. The experimentally generated waves were five JONSWAP-based waves with different peak periods and heights, propagating in three different water depths. The different depths allowed the investigation of three submergence depths (R_c) over the breakwaters and three local structure depths (d). In total, 15 experiments were conducted for each breakwater section. Other wave characteristics such as wave lengths over breakwaters' crests (L_p) were calculated according to the linear wave theory. The incident (H_i) transmitted (H_t), and reflected (H_r) wave heights were separated and estimated. The corresponding transmission (K_t), reflection (K_r), and dissipation coefficients (K_d) were calculated.

The variations of K_t and K_r for four rectangular sections against classic two-term dimensionless parameters were evaluated. Although the results showed that K_t and K_r variations were significantly sensitive to R_c/d, three dimensionless parameters of R_c/H_i, H_i/L and R_c/B were also effective. In this study, efforts were made to develop a comprehensive dimensionless parameter (based on the four abovementioned simple parameters) determining the transmission, reflection, and dissipation performances of investigated sections. It was found that the composite and uncomplicated parameter of $\beta = (R_c^2 L^{0.5}/dH_i B^{0.5})$ is an appropriate descriptive option to estimate the hydraulic responses of rectangular sections. Using this parameter, a unique ascending logarithmic curve against the increase of β could be fitted to the transmission coefficients of all rectangular sections in different water depths with $R^2 = 0.97$. In contrast, a descending logarithmic trend was fitted to all the observed reflection coefficients with $R^2 = 0.86$. The sensitivity of the transmission coefficient against β variations was approximately two times higher than that of the reflection coefficient. No exceptive assumptions and limiting categories are necessary to utilize the β parameter.

The reliability and capability of the proposed parameter were assessed using the results of trapezoidal section breakwater and compared with Van der Meer et al. (2005) relationships and results of Carevic et al. (2013). It was shown that the application of β was also valid for the trapezoidal section with all of the correlation coefficients and R-squared values greater than 0.92. However, the obtained fitted curve relationships were different from those of rectangle sections due to the geometric differences. Negligible differences between observed K_t values (pertaining to the experimental trapezoidal section) and predicted ones were found when using the three-formulation relationship of Van der Meer et al. (2005) showing the reliability of measured data and β formulation capability. Applying the β formulation for Carevic et al. (2013) measurements resulted in high $R^2 = 0.88$ for the fitted logarithmic curve. The proposed formulation predicting the transmission coefficients showed a strong agreement with some of the values resulting from formulations proposed by Van der Meer et al. (2005) for Carevic et al. (2013) data set. Comprising of one simple equation and with no concerns about discontinuity, these are the advantages of the newly proposed formulation. Finally, the simplicity and reliability of β application in determining submerged break-

water dimensions were demonstrated. As a secondary result, it was found that a rectangular section is more efficient than a trapezoidal section with the same upper side width.

Acknowledgments

The authors want to express their appreciation to Dr. P. Badiei from Department of Civil Engineering, Tehran University for his supports of this study.

References

Bao, T.Q., 2011. Effect of mangrove forest structures on wave attenuation in coastal Vietnam. Oceanologia 53 (3), 807—818. https://doi.org/10.5697/oc.53-3.807

Bleck, M., Oumeraci, H., 2002. Wave damping and spectral evolution at artificial reefs. In: Fourth International Symposium on Ocean Wave Measurement and Analysis, 1062—1072. https://doi.org/10.1061/40604(273)108

Carevic, D., Loncar, G., Prsic, M., 2012. Transformation of statistical and spectral wave periods crossing a smooth low-crested structure. Oceanologia 54 (1), 39—58. https://doi.org/10.5697/oc.54-1.039

Carevic, D., Loncar, G., Prsic, M., 2013. Wave parameters after smooth submerged breakwater. Coastal Eng 79, 32—41. https://doi.org/10.1016/j.coastaleng.2013.04.004

Dattatri, J., Raman, H., Shankar, N.J., 1978. Performance characteristics of submerged breakwaters. In: Proc. 16th Int. Conf. on Coastal Eng, 1978, 2153—2171. https://doi.org/10.9753/icce.v16.130

d'Angremond, K., Van der Meer, J.W., de Jong, R.J., 1996. Wave transmission at low crested structures. In: Proc. 25th Int. Conf. on Coastal Eng. ASCE, 3305—3318. https://doi.org/10.1061/9780784402429.187

Davidson, M., Bird, P., Bullock, G., Huntley, D., 1996. A new non-dimensional number for the analysis of wave reflection from rubble mound breakwaters. Coastal Eng 28, 93—120. https://doi.org/10.1016/0378-3839(96)00012-9

Dean, R.G., Chen, R., Browder, A.E., 1997. In: Full scale monitoring study of a submerged breakwater. Palm Beach, Florida, USA. Coastal Eng. 29, 291—315. https://doi.org/10.1016/S0378-3839(96)00028-2

Fang, Z., Xiao, L., Kou, Y., Li, J., 2018. Experimental study of the wave-dissipating performance of a four-layer horizontal porous-plate breakwater. Ocean Eng. 151, 222—233. https://doi.org/10.1016/j.oceaneng.2018.01.041

Filianoti, P., Piscopo, R., 2015. Sea wave energy transmission behind submerged absorber caissons. Ocean Eng. 93, 107—117. https://doi.org/10.1016/j.oceaneng.2014.09.031

Gao, J., Ma, X., Zang, J., Dong, G., Ma, X., Zhu, Y., Zhou, L., 2020. Numerical investigation of harbor oscillations induced by focused transient wave groups. Coastal Eng 158, 103670. https://doi.org/10.1016/j.coastaleng.2020.103670

Gao, J., Zhou, X., Zhou, L., Zang, J., Chen, H., 2019. Numerical investigation on effects of fringing reefs on low-frequency oscillations within a harbor. Ocean Eng 172, 86—95. https://doi.org/10.1016/j.oceaneng.2018.11.048

Goda, Y., Suzuki, Y., 1976. Estimation of incident and reflected waves in random wave experiments. Coastal Eng 1976, 828—845. https://doi.org/10.9753/icce.v15.47

Goda, Y., Takeda, H., Moriya, Y., 1967. Laboratory investigation on wave transmission over breakwaters. Port Harbour Tech. Res. Inst

Hajivalie, F., Mahmoudof, S.M., 2018. Experimental Study of Energy Dissipation at Rectangular Submerged Breakwater. In: Proc. of ICFM8. Sendai, Japan.

Hajivalie, F., Yeganeh-Bakhtiary, A., Bricker, J.D., 2015. Numerical study of the effect of submerged vertical breakwater dimension on wave hydrodynamics and vortex generation. Coastal Eng. J. 57 (03), 1550009. https://doi.org/10.1142/S0578563415500096

Kubowicz-Grajewska, A., 2015. Morpholithodynamical changes of the beach and the nearshore zone under the impact of submerged breakwaters—a case study (Orłowo Cliff, the Southern Baltic). Oceanologia 57 (2), 144—158. https://doi.org/10.1016/j.oceano.2015.01.002

Liang, B., Wu, G., Liu, F., Fan, H., Li, H., 2015. Numerical study of wave transmission over double submerged breakwaters using non-hydrostatic wave model. Oceanologia 57 (4), 308—317. https://doi.org/10.1016/j.oceano.2015.07.002

Liao, Y.-C., Jiang, J.-H., Wu, Y.-P., Lee, C.-P., 2013. Experimental study of wave breaking criteria and energy loss caused by a submerged porous breakwater on horizontal bottom. J. Mar. Sci. Technol. 21 (1), 35—41. https://doi.org/10.6119/JMST-011-0729-1

Liu, Y., Li, H.-J., 2012. Analysis of wave interaction with submerged perforated semi-circular breakwaters through multipole method. Appl. Ocean Res. 34, 164—172. https://doi.org/10.1016/j.apor.2011.08.003

Lokesh, K.N.B., Sannasiraj, S., Sundar, V., Schlurmann, T., 2015. Experimental investigations on wave transmission at submerged breakwater with smooth and stepped slopes. Procedia Eng. 116 (1), 713—719. https://doi.org/10.1016/j.proeng.2015.08.356

Lorenzoni, C., Piattella, A., Soldini, L., Mancinelli, A., Brocchini, M., 2015. An experimental investigation of the hydrodynamic circulation in the presence of submerged breakwaters, Proc. 5th International Symposium on Ocean Measurements and Analysis, Paper no. 125.

Lorenzoni, C., Postacchini, M., Brocchini, M., Mancinelli, A., 2016. Experimental study of the short-term efficiency of different breakwater configurations on beach protection. J. Ocean Eng. Mar. Energy 2 (2), 195—210. https://doi.org/10.1007/s40722-016-0051-9

Mahmoudof, S.M., Azizpour, J., 2020. Field observation of wave reflection from plunging cliff coasts of Chabahar. Appl. Ocean Res. 95, 102029. https://doi.org/10.1016/j.apor.2019.102029

Mansard, E.P., Funke, E., 1980. The measurement of incident and reflected spectra using a least squares method. In: Proc. 17th Int. Conf. on Coastal Eng, 1980, 154—172. https://doi.org/10.9753/icce.v17.8

Rageh, O., Koraim, A., 2010. Hydraulic performance of vertical walls with horizontal slots used as breakwater. Coastal Eng 57 (8), 745—756. https://doi.org/10.1016/j.coastaleng.2010.03.005

Rao, S., Shirlal, K.G., Varghese, R.V., Govindaraja, K., 2009. Physical model studies on wave transmission of a submerged inclined plate breakwater. Ocean Eng 36 (15—16), 1199—1207. https://doi.org/10.1016/j.oceaneng.2009.08.001

Sindhu, S., Shirlal, K.G., 2015. Prediction of wave transmission characteristics at submerged reef breakwater. Procedia Eng. 116, 262—268. https://doi.org/10.1016/j.proeng.2015.08.289

Suh, K.D., Choi, J.C., Kim, B.H., Park, W.S., Lee, K.S., 2001. Reflection of irregular waves from perforated-wall caisson breakwaters. Coastal Eng 44 (2), 141—151. https://doi.org/10.1016/S0378-3839(01)00028-X

Sumer, B.M., Fredsøe, J., Lamberti, A., Zanuttigh, B., Dixen, M., Gislason, K., Di Penta, A.F., 2005. Local scour at roundhead and along the trunk of low crested structures. Coastal Eng 52 (10—11), 995—1025. https://doi.org/10.1016/j.coastaleng.2005.09.012

Van der Meer, J.W., 1991. Stability and transmission at low-crested structures. Delft Hydraulics Publ.

Van der Meer, J.W., Briganti, R., Zanuttigh, B., Wang, B., 2005. Wave transmission and reflection at low-crested structures: Design formulae, oblique wave attack and spectral change. Coastal Eng 52 (10—11), 915—929. https://doi.org/10.1016/j.coastaleng.2005.09.005

Young, D.M., Testik, F.Y., 2011. Wave reflection by submerged vertical and semicircular breakwaters. Ocean Eng 38 (10), 1269—1276. https://doi.org/10.1016/j.oceaneng.2011.05.003

Zhang, N., Zhang, Q., Zou, G., Jiang, X., 2016. Estimation of the transmission coefficients of wave height and period after smooth submerged breakwater using a non-hydrostatic wave model. Ocean Eng 122, 202—214. https://doi.org/10.1016/j.oceaneng.2016.06.037